OPTICA

PUBLISHING GROUP

Formerly OSA

Actively Q-switched radially polarized Ho:YAG laser with an intra-cavity laser-written S-waveplate

Matthew J. Barber[1,*], Peter C. Shardlow[1], Yuhao Lei[1], Peter G. Kazansky[1], and W. Andrew Clarkson[1]

[1]Optoelectronics Research Centre, University of Southampton, Southampton, SO17 1BJ, United Kingdom
*Corresponding author: m.j.barber@soton.ac.uk

Nanosecond Q-switched pulses and radial polarization are established standalone techniques for enhanced laser materials processing applications, but are generally challenging to achieve simultaneously at high average power levels. Here, we demonstrate a 20.6 W radially polarized Ho:YAG rod laser which has been actively Q-switched in order to generate 515 µJ, 210 ns pulses at 2097 nm. By utilizing an ultra-low-loss spatially-variant birefringent waveplate (S-waveplate) inside the laser cavity, the linearly polarized fundamental mode has been converted to a radially polarized donut-shaped beam with very high conversion efficiency. © 2022 Optica Publishing Group

High power laser sources operating in the 2.1 µm wavelength regime are attractive for use in a variety of applications such as defensive countermeasures, surgical treatment and materials processing [1–4]. Although the output power and wavelength are often critical parameters for suitable design of the laser, the system can be optimized even further by manipulating optical characteristics such as the beam shape, polarization distribution and temporal dynamics. To this end, Q-switched pulsed lasers are a very common choice for materials processing applications, as the rapid (nanosecond-scale) delivery of beam energy to the material can produce a smaller heat affected zone and higher finish quality than an equivalent continuous-wave laser [5]. In particular, nanosecond-scale pulse durations are well suited to the cutting, drilling and welding of materials as there is sufficient time for the illuminated region to melt significantly during the pulse arrival window, in contrast to the ablation-based process of picosecond and femtosecond machining lasers [6].

Laser materials processing can also benefit greatly from the use of radially polarized light, where the polarization vector at each position in the beam profile points outwards from the central intensity minimum. Such a polarization state is able to produce increased beam absorption and a higher cutting efficiency at the large angles of incidence typically encountered, due to the establishment of p-polarized illumination across most of the cutting zone [7, 8]. As such, the combination of radial polarization and cavity Q-switching can offer additional system flexibility and a number of attractive benefits for laser materials processing, in comparison to the use of radial polarization or Q-switching alone.

At present, up to 3.9 W of radially polarized Q-switched operation has been reported using polarization discrimination techniques such as birefringent crystals and photonic crystal grating mirrors, or by exploiting the thermally-induced stress birefringence and bifocusing within the pumped gain medium [9–12]. However, these approaches have typically relied upon saturable absorbers in order to achieve passive Q-switching of the laser cavity, limiting any control on the output pulse characteristics. Actively Q-switched radially polarized emission has previously been demonstrated in a 4.6 W Nd:YAG laser which utilized gain medium thermally-induced bifocusing and a polarization-insensitive acousto-optic modulator [13], but this approach is usually restricted to only generate a high purity radially polarized emission for a very limited range of output power levels.

Recent developments in the generation of radially polarized light have explored the use of laser-written spatially-variant birefringent waveplates (S-waveplates) [14, 15]. Such devices utilize a two-dimensional array of sub-micron-sized waveplates where the slow axis varies in accordance with the azimuthal angle. In general, the waveplate array is produced by making a nanogratings-based birefringence modification directly to a fused silica substrate [16], which results in a very high damage threshold fluence and thus makes the S-waveplate particularly attractive for use in high-energy Q-switched laser operation. The implementation of S-waveplates for radially polarized beam generation has been demonstrated within the laser cavity of a gain-switched Yb-doped fiber laser, achieving up to 22.5 W of average output power [17]. More recently, an ultra-low-loss anisotropic-nanopores-based birefringent modification (type X) has been demonstrated by femtosecond laser direct writing in silica glass [18]. This approach is more appealing for use with an intra-cavity S-waveplate due to the less than 1% scattering loss that can be achieved and the presence of an even higher damage threshold than existing type II birefringent modification techniques [19, 20].

Here, we demonstrate a novel power-scalable approach for the generation of Q-switched laser emission with a radially
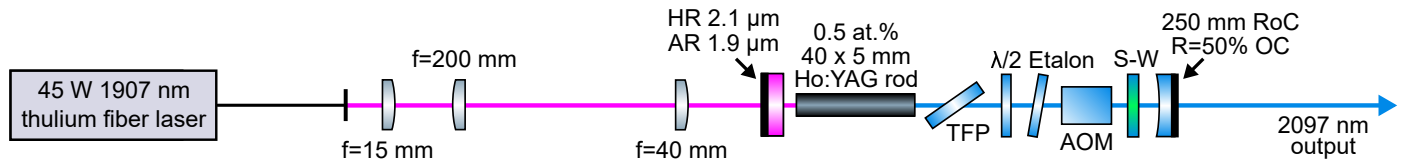
Fig. 1. Optical schematic of the radially polarized Q-switched Ho:YAG laser, containing a thin film polarizer (TFP), half-wave plate (λ/2), acousto-optic modulator (AOM) and S-waveplate (S-W).

polarized output profile, using an intra-cavity S-waveplate to convert the linearly polarized fundamental (LG$_{00}$) mode into a beam with radial polarization prior to the output coupler. The S-waveplate had a very high conversion efficiency from linear to radial polarization and was fabricated based on an ultra-low-loss anisotropic nanopores birefringent modification within a silica glass substrate by ultrafast laser writing. The 20.6 W Ho:YAG rod laser was actively Q-switched using a fused quartz acousto-optic modulator (AOM), achieving a pulse energy of 515 µJ and a pulse duration of 210 ns (FWHM) at a repetition rate of 40 kHz, with the output power limited by the available pump power.

A two-mirror linear laser cavity was constructed between a plane-parallel input coupler mirror and a plano-concave output coupler, as illustrated in Fig. 1. Here, the input coupler was highly reflective (HR) at 2.1 µm and anti-reflection (AR) coated at 1.9 µm, while the output coupler was partially reflective (R = 50%) at the 2.1 µm lasing wavelength and had a 250 mm radius of curvature. The laser cavity included a 40 mm long Ho:YAG rod crystal with a 5 mm diameter and 0.5 at.% doping concentration, which was positioned near the input coupler end of the cavity. The rod was AR-coated on both end faces for 1.9 and 2.1 µm, and mounted in a water-cooled copper heat-sink maintained at 20°C. The Ho:YAG laser was aligned for operation on the fundamental LG$_{00}$ (Laguerre-Gaussian) cavity mode at a physical resonator length of 190 mm.

A thin-film polarizer (TFP, Layertec, >200:1 extinction ratio) was utilized after the Ho:YAG rod in order to generate linearly polarized light within the cavity, as required for high efficiency conversion to a radially polarized beam by the S-waveplate. The linear polarization was then rotated from the horizontal (x) to vertical (y) direction by a half-wave plate (Union Optic) as required for maximum diffraction efficiency in the acousto-optic modulator Q-switch. To prevent laser emission at both gain peaks of Ho:YAG (2090 nm and 2097 nm), a 100 µm-thick YAG etalon (Layertec) was added to the cavity and its angle adjusted to select 2097 nm as the lone emission wavelength. To produce Q-switched pulses, a fused quartz AOM (Gooch & Housego) was used with 50 W RF drive power at 40.68 MHz and with both end faces AR coated at 1.9–2.1 µm. Lastly, the in-house fabricated S-waveplate was positioned within the cavity before the output coupler mirror. The S-waveplate was held in a rotation mount to ensure that the birefringent nanostructures could be appropriately aligned with respect to the incident linear polarization vector for conversion into a radially polarized beam.

The S-waveplate had a diameter of 3 mm and was fabricated by birefringence patterning in an infrared-grade fused silica glass substrate (Suprasil 300) using an ultrafast laser operating at a wavelength of 1030 nm and with a pulse duration of 600 fs. The S-waveplate retardance was set to half the wavelength of 2097 nm, and the slow axis azimuth was half of the polar angle. The writing conditions, objective numerical aperture of 0.16, pulse energy and scanning speed were chosen in such a way as to

obtain a birefringent modification in the silica glass with random anisotropic nanopores, which is characterized by ultrahigh beam transmission. The measured transmission of the manufactured type X S-waveplate with reference to an untreated quartz glass sample at a wavelength of 2097 nm exceeded 99% (excluding the loss contribution due to Fresnel reflection from the end faces), whilst the damage threshold was around 1.56 J/cm^2 for a 1030 nm, 300 fs incident beam, which is 1.6 times higher than for a type II S-waveplate. Depending on the polarization azimuth of the input Gaussian beam, a radially or azimuthally polarized vector beam with good contrast and uniformity is generated, while a vortex beam can be produced for an circularly polarized input beam. After fabrication, the S-waveplate was AR-coated on both sides for 2.1 µm light.

The Ho:YAG rod laser was single-end-pumped by a 45 W, 1907 nm thulium-doped fiber laser which generated a robustly fundamental-mode emission profile and was removed of any residual 793 nm pump light by a cladding mode stripper. The 1907 nm output beam was collimated by a f=15 mm lens and then passed through a 5-times demagnification telescope formed from a f=200 mm and f=40 mm plano-convex lens pair. Such conditioning produced an approximately-collimated pump beam diameter of 720 µm along the length of the crystal, with most residual pump light being reflected out of the cavity by the TFP.

The Q-switched Ho:YAG laser was initially operated at a 40 kHz repetition rate and a 12% AOM-open duty cycle, generating an output power of up to 20.6 W and a corresponding pulse energy of 515 µJ (Fig. 2). The 20.6 W emission was achieved with
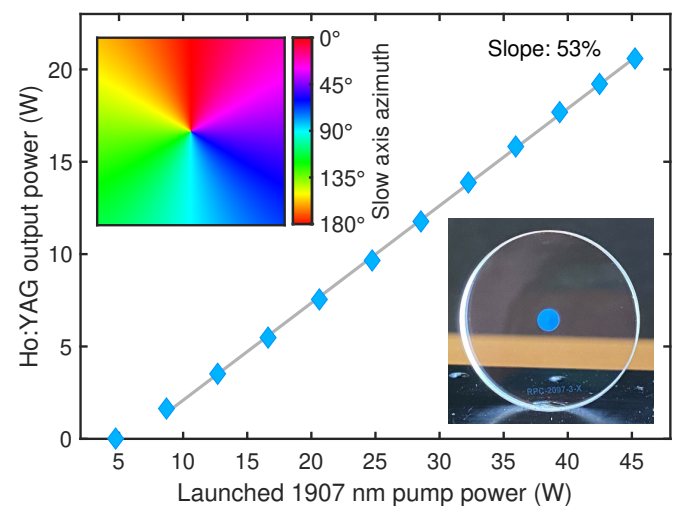

Fig. 2. Output power curve for the Q-switched Ho:YAG laser at a 40 kHz repetition rate. Inset, top-left: Exemplar variation of the slow axis azimuth across an S-waveplate. Inset, bottom-right: Photograph of the fabricated S-waveplate.

a 53% slope efficiency with respect to launched pump power, a 6 W threshold and an estimated 5 W of unabsorbed pump power. The laser output power was limited by the available 1907 nm pump power. An exemplar 2D illustration of the variation in the slow axis azimuth with respect to the horizontal plane across a polarization-converting S-waveplate is shown as an inset of Fig. 2, accompanied by an image of the fabricated S-waveplate that has been used inside the Ho:YAG laser cavity. The temporal characteristics of the Q-switched Ho:YAG laser were analyzed using an extended InGaAs photodetector (Hamamatsu) with a 7 ns rise time. To this end, the single pulse trace and generated pulse train for 20.6 W of emission at a 40 kHz repetition rate are shown in Fig. 3a and 3b respectively, with no pulse skipping observed during full power operation and no pre-lasing detected between the individual 25 μs-spaced pulses.

The laser emission spectrum was measured at the maximum incident pump power using a Yokogawa AQ6375B spectrum analyzer, demonstrating laser output entirely at 2097 nm (Fig. 3c), as dictated by the intra-cavity YAG etalon. The variation in the pulse energy and pulse duration for a selection of repetition rates between 40 and 70 kHz is shown in Fig. 3d, spanning 515 to 295 μJ and 210 to 416 ns across this range, with the AOM duty cycle re-optimized for each repetition rate value to retain clean pulse generation. Shorter output pulse durations and higher peak power levels could be achieved with further reduction of the AOM repetition rate, whilst ensuring that the laser remains suitably far below the dielectric coating damage intensity threshold.

The output beam intensity profile at maximum pump power was captured with a microbolometer camera (FLIR Lepton 3.0) before and after introduction of the S-waveplate to the cavity, as shown in Fig. 4. Here, the relatively uniform donut-shaped profile that is generated when the S-waveplate is in use indicates that very little beam distortion has been imparted onto the laser during transmission through the polarization converting device, with any small substructures of the beam profile attributed to imperfections and defects produced during fabrication of the S-waveplate. Furthermore, no detectable power change was observed after the S-waveplate had been placed into the cavity,
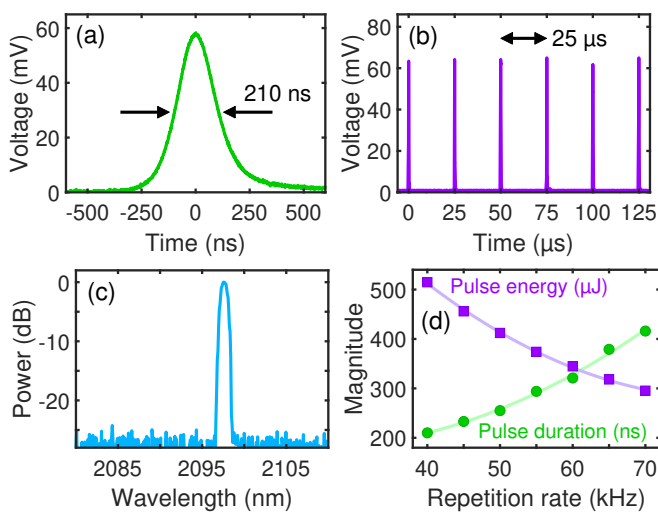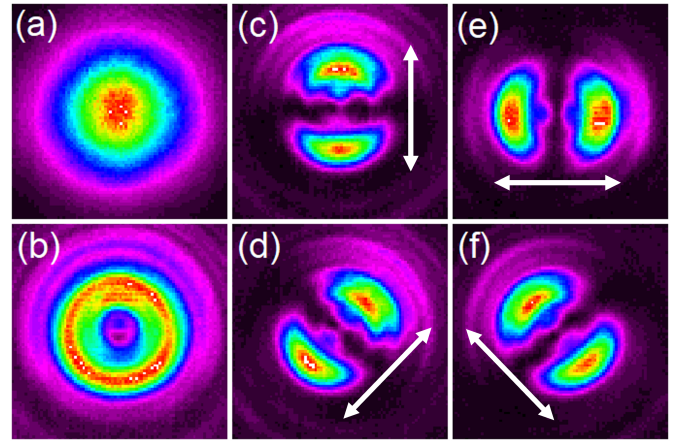

Fig. 4. Beam intensity profiles of the Ho:YAG laser output (a) without and (b) with the S-waveplate inside the cavity. (c)-(f) Images of the radially polarized laser emission when passed through a linear polarization filter, with the transmission axis indicated by the annotated arrows.

suggesting that the scattering losses of the type X birefringent modification are very low in the 2.1 μm regime. The slightly imperfect central region of the donut-shaped beam is likely to arise due to the need to fabricate a significant change in slow axis angle across a very small spatial distance either side of the central singularity, which can be seen from the top-left inset of Fig. 2. In addition, this region requires the S-waveplate to achieve total extinction of the most intense part of the incident beam, such that even a relatively small amount of imperfect conversion will be more noticeable here than in the rest of the donut-shaped profile.

The radial polarization purity of the Ho:YAG laser emission was measured by passing a sample of the beam through an absorptive linear polarizer placed before the imaging camera (with an extinction ratio exceeding 10,000:1), generating a two-lobe intensity profile that is aligned with the transmission axis of the linear filter. By tracing the intensity variation along a circular path which intersects the maximum of each lobe, the ratio between the maximum and minimum intensity regions of the trace can be calculated and defined as the radial polarization purity [21]. By then repeating the two-lobe intensity variation analysis for multiple orientations of the polarizer and averaging across the measurement, the radial polarization of the overall output beam was determined to be 49:1, which indicates a high purity radially polarized output. The two-lobe intensity profiles corresponding to filter angles of 0°, 45°, 90° and 135° with respect to the vertical axis are shown in Fig. 4c–f.

The absence of light detected across the middle of Fig. 4c suggests that very little of the original vertically polarized LG_{00} mode has been transmitted through the S-waveplate and therefore the intrinsic polarization conversion efficiency of the S-waveplate is very high. Although the type X birefringence modification generally has very low dispersion, the Ho:YAG laser operating wavelength of 2097 nm is much longer than the 546 nm wavelength used to characterize the birefringence after fabrication. As a result, the potential presence of some weak dispersion in the S-waveplate may have contributed to any slightly imperfect conversion of the linearly polarized light into a radially polarized beam. However, the conversion performance can be further optimized by precise high-temperature annealing

Fig. 3. (a) Single pulse trace, (b) pulse train and (c) emission spectrum of the radially polarized Q-switched Ho:YAG laser operating at 40 kHz. (d) Variation in the output pulse energy and pulse duration as a function of the AOM repetition rate.

of the S-waveplate in order to tune the birefringence to the desired magnitude during illumination with a suitable 2097 nm probe beam.

An evaluation of the laser's beam propagation factor (M^2) at the maximum pump power was performed using an Ophir Nanoscan scanning-slit profiler, for the laser system with and without the S-waveplate inside the resonator. In the absence of the S-waveplate, the M^2 values were measured to be 1.10 and 1.09 in the horizontal (x) and vertical (y) directions respectively, indicating a robust fundamental LG_{00} output mode from the laser. In addition, M^2 values of 2.14 and 2.12 were observed in the horizontal and vertical directions respectively when the S-waveplate was placed inside the resonator, which are only slightly larger than the theoretical value of 2 for a perfect radially polarized LG_{01} mode.

In summary, we have reported on the development of a 20.6 W actively Q-switched Ho:YAG laser with a radially polarized output by way of an intra-cavity laser-written spatially-variant waveplate (S-waveplate). For a repetition rate of 40 kHz, the Q-switched laser produced a maximum pulse energy of 515 µJ with a pulse duration of 210 ns and a corresponding peak power of 2.5 kW, limited by the maximum output power of the 1907 nm thulium fiber laser pump source. While a radially polarized laser which uses gain medium bifocusing would have radial polarization at all positions within the cavity, our approach only generates radial polarization in a small section of the cavity, permitting the use of a standard acousto-optic modulator in the linearly polarized part of the resonator. Due to the combination of a high damage threshold, low scattering losses and the ability to fabricate larger-diameter polarization converting devices, the S-waveplate-based approach demonstrated here should readily enable much greater output power scaling and the generation of very high pulse energy emission without compromising radial polarization purity.

Disclosures. The authors declare no conflicts of interest.

Data availability. The data underpinning this publication is available from the University of Southampton repository at https://doi.org/10.5258/SOTON/D2236.

REFERENCES

1. B.-R. Zhao, B.-Q. Yao, C.-P. Qian, G.-Y. Liu, Y. Chen, R.-X. Wang, T.-Y. Dai, and X.-M. Duan, Opt. Lett. **43**, 5989 (2018).
2. A. Leunig, P. Janda, R. Sroka, R. Baumgartner, and G. Grevers, The Laryngoscope **109**, 1690 (1999).
3. I. Astrauskas, B. Považay, A. Pugžlys, and A. Baltuška, "Material Processing with Picosecond 2-µm Pulses from Ho:YAG Amplifier," in *Laser Congress 2019 (ASSL, LAC, LS&C),* (OSA, Washington, D.C., 2019), p. AW4A.6.
4. I. Mingareev, F. Weirauch, A. Olowinsky, L. Shah, P. Kadwani, and M. Richardson, Opt. & Laser Technol. **44**, 2095 (2012).
5. F. Olsen and L. Alting, CIRP Annals **44**, 141 (1995).
6. Y. L. Yao, H. Chen, and W. Zhang, The Int. J. Adv. Manuf. Technol. **26**, 598 (2005).
7. V. G. Niziev and A. V. Nesterov, J. Phys. D: Appl. Phys. **32**, 1455 (1999).
8. R. Weber, A. Michalowski, M. Abdou-Ahmed, V. Onuseit, V. Rominger, M. Kraus, and T. Graf, Phys. Procedia **12**, 21 (2011).
9. X. Sun, Y. Wu, S. Chen, and J. Li, Laser Phys. **28**, 055103 (2018).
10. D. Lin, K. Xia, R. Li, X. Li, G. Li, K.-i. Ueda, and J. Li, Opt. Lett. **35**, 3574 (2010).
11. L. Li, X. Zheng, C. Jin, M. Qi, X. Chen, Z. Ren, J. Bai, and Z. Sun, Appl. Phys. Lett. **105**, 221103 (2014).
12. Zhiqiang Fang, Kegui Xia, Yao Yao, and Jianlang Li, IEEE J. Sel. Top. Quantum Electron. **21**, 337 (2015).
13. M. Meier, V. Romano, and T. Feurer, Appl. Phys. A **86**, 329 (2007).
14. M. Beresna, M. Gecevičius, and P. G. Kazansky, Opt. Mater. Express **1**, 783 (2011).
15. R. Drevinskas and P. G. Kazansky, APL Photonics **2**, 066104 (2017).
16. S. Richter, M. Heinrich, S. Döring, A. Tünnermann, S. Nolte, and U. Peschel, J. Laser Appl. **24**, 042008 (2012).
17. D. Lin, N. Baktash, M. Berendt, M. Beresna, P. G. Kazansky, W. A. Clarkson, S. U. Alam, and D. J. Richardson, Opt. Lett. **42**, 1740 (2017).
18. M. Sakakura, Y. Lei, L. Wang, Y.-H. Yu, and P. G. Kazansky, Light. Sci. & Appl. **9**, 15 (2020).
19. T. L. Jefferson-Brain, Y. Lei, P. G. Kazansky, and W. A. Clarkson, "Generation of a Radially Polarised Beam in a Solid-State Laser Using an Intracavity Spatially Variant Waveplate," in *2021 Conference on Lasers and Electro-Optics Europe & European Quantum Electronics Conference (CLEO/Europe-EQEC),* (2021), p. CA_8_3.
20. X. Chang, Y. Lei, H. Wang, G. Shayeganrad, C. Deng, and P. Kazansky, "High Damage Threshold Ultrafast Laser Nanostructuring in Silica Glass," in *2021 Conference on Lasers and Electro-Optics Europe & European Quantum Electronics Conference (CLEO/Europe-EQEC),* (IEEE, 2021), pp. 1–1.
21. D. Lin, J. M. O. Daniel, M. Gecevičius, M. Beresna, P. G. Kazansky, and W. A. Clarkson, Opt. Lett. **39**, 5359 (2014).

Full references:

1. B.-R. Zhao, B.-Q. Yao, C.-P. Qian, G.-Y. Liu, Y. Chen, R.-X. Wang, T.-Y. Dai, and X.-M. Duan, "231 W dual-end-pumped Ho:YAG MOPA system and its application to a mid-infrared ZGP OPO", Optics Letters, 43, 5989 (2018).

2. A. Leunig, P. Janda, R. Sroka, R. Baumgartner, and G. Grevers, "Ho:YAG Laser Treatment of Hyperplastic Inferior Nasal Turbinates", The Laryngoscope, 109, 1690 (1999).

3. I. Astrauskas, B. Považay, A. Pugžlys, and A. Baltuška, "Material Processing with Picosecond 2-μm Pulses from Ho:YAG Amplifier" in Laser Congress 2019 (ASSL, LAC, LS&C), (OSA, Washington, D.C., 2019), p. AW4A.6.

4. I. Mingareev, F. Weirauch, A. Olowinsky, L. Shah, P. Kadwani, and M. Richardson, "Welding of polymers using a 2μm thulium fiber laser", Optics & Laser Technology, 44, 2095 (2012).

5. F. Olsen and L. Alting, "Pulsed Laser Materials Processing, ND-YAG versus CO_2 Lasers", CIRP Annals, 44, 141 (1995).

6. Y. L. Yao, H. Chen, and W. Zhang, "Time scale effects in laser material removal: a review", The International Journal of Advanced Manufacturing Technology, 26, 598 (2005).

7. V. G. Niziev and A. V. Nesterov, "Influence of beam polarization on laser cutting efficiency", Journal of Physics D: Applied Physics, 32, 1455 (1999).

8. R. Weber, A. Michalowski, M. Abdou-Ahmed, V. Onuseit, V. Rominger, M. Kraus, and T. Graf, "Effects of Radial and Tangential Polarization in Laser Material Processing", Physics Procedia, 12, 21 (2011).

9. X. Sun, Y. Wu, S. Chen, and J. Li, "Radially polarized and passively Q -switched Yb-doped fiber laser based on intracavity birefringent mode discrimination", Laser Physics, 28, 055103 (2018).

10. D. Lin, K. Xia, R. Li, X. Li, G. Li, K.-i. Ueda, and J. Li, "Radially polarized and passively Q-switched fiber laser", Optics Letters, 35, 3574 (2010).

11. L. Li, X. Zheng, C. Jin, M. Qi, X. Chen, Z. Ren, J. Bai, and Z. Sun, "High repetition rate Q-switched radially polarized laser with a graphene-based output coupler", Applied Physics Letters, 105, 221103 (2014).

12. Zhiqiang Fang, Kegui Xia, Yao Yao, and Jianlang Li, "Radially Polarized and Passively Q-Switched Nd:YAG Laser Under Annular-Shaped Pumping", IEEE Journal of Selected Topics in Quantum Electronics, 21, 337 (2015).

13. M. Meier, V. Romano, and T. Feurer, "Material processing with pulsed radially and azimuthally polarized laser radiation", Applied Physics A, 86, 329 (2007).

14. M. Beresna, M. Gecevicius, and P. G. Kazansky, "Polarization sensitive elements fabricated by femtosecond laser nanostructuring of glass [Invited]", Optical Materials Express, 1, 783 (2011).

15. R. Drevinskas and P. G. Kazansky, "High-performance geometric phase elements in silica glass", APL Photonics, 2, 066104 (2017).

16. S. Richter, M. Heinrich, S. Döring, A. Tünnermann, and S. Nolte, "Nanogratings in fused silica: Formation, control, and applications", Journal of Laser Applications, 24, 042008 (2012).

17. D. Lin, N. Baktash, M. Berendt, M. Beresna, P. G. Kazansky, W. A. Clarkson, S. U. Alam, and D. J. Richardson, "Radially and azimuthally polarized nanosecond Yb-doped fiber MOPA system incorporating temporal shaping", Optics Letters, 42, 1740 (2017).

18. M. Sakakura, Y. Lei, L. Wang, Y.-H. Yu, and P. G. Kazansky, "Ultralow-loss geometric phase and polarization shaping by ultrafast laser writing in silica glass", Light: Science & Applications, 9, 15 (2020).

19. T. L. Jefferson-Brain, Y. Lei, P. G. Kazansky, and W. A. Clarkson, "Generation of a Radially Polarised Beam in a Solid-State Laser Using an Intracavity Spatially Variant Waveplate" in 2021 Conference on Lasers and Electro-Optics Europe & European Quantum Electronics Conference (CLEO/Europe-EQEC), (2021), p. CA_8_3.

20. X. Chang, Y. Lei, H. Wang, G. Shayeganrad, C. Deng, and P. G. Kazansky, "High Damage Threshold Ultrafast Laser Nanostructuring in Silica Glass" in 2021 Conference on Lasers and Electro-Optics Europe & European Quantum Electronics Conference (CLEO/Europe-EQEC), (2021), p. 1-1.

21. D. Lin, J. M. O. Daniel, M. Gecevicius, M. Beresna, P. G. Kazansky and W. A. Clarkson, "Cladding-pumped ytterbium-doped fiber laser with radially polarized output", Optics Letters, 39, 5359 (2014).